

## Temperature Sensors Integrated into a CMOS Image Sensor

Abarca, Accel; Xie, Shuang; Markenhof, Jules; Theuwissen, Albert

**DOI**

[10.3390/proceedings1040358](https://doi.org/10.3390/proceedings1040358)

**Publication date**

2017

**Document Version**

Final published version

**Published in**

Proceedings of Eurosensors 2017

**Citation (APA)**

Abarca, A., Xie, S., Markenhof, J., & Theuwissen, A. (2017). Temperature Sensors Integrated into a CMOS Image Sensor. In *Proceedings of Eurosensors 2017* (pp. 358-361). (Proceedings; Vol. 1, No. 4). <https://doi.org/10.3390/proceedings1040358>

**Important note**

To cite this publication, please use the final published version (if applicable). Please check the document version above.

**Copyright**

Other than for strictly personal use, it is not permitted to download, forward or distribute the text or part of it, without the consent of the author(s) and/or copyright holder(s), unless the work is under an open content license such as Creative Commons.

**Takedown policy**

Please contact us and provide details if you believe this document breaches copyrights. We will remove access to the work immediately and investigate your claim.

Proceedings

# Temperature Sensors Integrated into a CMOS Image Sensor <sup>†</sup>

Accel Abarca <sup>1,\*</sup>, Shuang Xie <sup>1</sup>, Jules Markenhof <sup>1</sup> and Albert Theuwissen <sup>1,2</sup>

<sup>1</sup> Electronic Instrumentation Laboratory, TU Delft, Delft, The Netherlands; s.xie@tudelft.nl (S.X.); j.markenhof@gmail.com (J.M.); a.theuwissen@scarlet.be (A.T.)

<sup>2</sup> Harvest Imaging, Bree, Belgium

\* Correspondence: a.n.abarcaprouza@tudelft.nl; Tel.: +31-15-27-86432

<sup>†</sup> Presented at the Eurosensors 2017 Conference, Paris, France, 3–6 September 2017.

Published: 9 September 2017

**Abstract:** In this work, a novel approach is presented for measuring relative temperature variations inside the pixel array of a CMOS image sensor itself. This approach can give important information when compensation for dark (current) fixed pattern noise (FPN) is needed. The test image sensor consists of pixels and temperature sensors pixels (=Tixels). The size of the Tixels is 11  $\mu\text{m} \times 11 \mu\text{m}$ . Pixels and Tixels are placed next to each other in the active imaging array and use the same readout circuits. The design and the first measurements of the combined image-temperature sensor are presented.

**Keywords:** pixels; bipolar based temperature sensors; dark current

---

## 1. Introduction

Dark current is one of the major contributors of FPN in image sensors. The amount of dark current highly depends on process variations as well as temperature variations. In the case of dark current-temperature relation, it has been reported that dark current doubles every 5 °C [1,2]. Different techniques are applied to compensate the non-uniformities of dark current, e.g., by means of a dark reference frame. But creating a dark reference frame requires a mechanical shutter in the camera. Integrating the temperature sensors allows measuring the relative temperature variations in-situ of the image sensor and this can be used to compensate for dark current FPN.

An image sensor consisting of 12,288 pixels has been designed and fabricated. The size of the image sensor is 64 rows by 192 columns. 555 pixels in the array were replaced by temperature sensors pixels. The Tixels are uniformly placed along the pixel array having 3 Tixels per row and 8 Tixels per column.

## 2. Description of the Test System

### 2.1. Pixels and Tixels

The pixels of the image sensor are based on a CMOS 4T architecture, as shown in Figure 1a. This architecture is highly used nowadays because it provides low noise, low dark current and high quantum efficiency due to the pinned photodiode—transfer gate—floating diffusion structure [3].

On the other hand, the temperature sensors are based on parasitic BJT and its schematic is shown in Figure 1b. In general, BJT based temperature sensors feature inherent better accuracy, fast measurements and lower process variations, compared to their CMOS based alternative [4,5]. The Tixel is composed of the BJT, a Tixel selector ( $CS_i$ ), a bias current and a source follower. Each Tixel is selected by the control signals  $CS_i$  and  $RS_j$ . Once  $CS_i$  is high, the BJT is biased by the currents

$I_{bias1}$  or  $I_{bias2}$  in a ratio 4:1 ( $I_{bias1}/I_{bias2}$ ). Then through the source follower the proportionality to absolute temperature (PTAT) is obtained via the differential Base-Emitter Voltage ( $\Delta V_{BE}$ ) characterization (Equation (1)):

$$\Delta V_{BE} = \frac{kT}{q} \ln(N), \tag{1}$$

where  $k$  corresponds to the Boltzmann constant,  $T$  is the absolute temperature,  $q$  is the electron charge, and  $N$  corresponds to the current ratio 4:1.

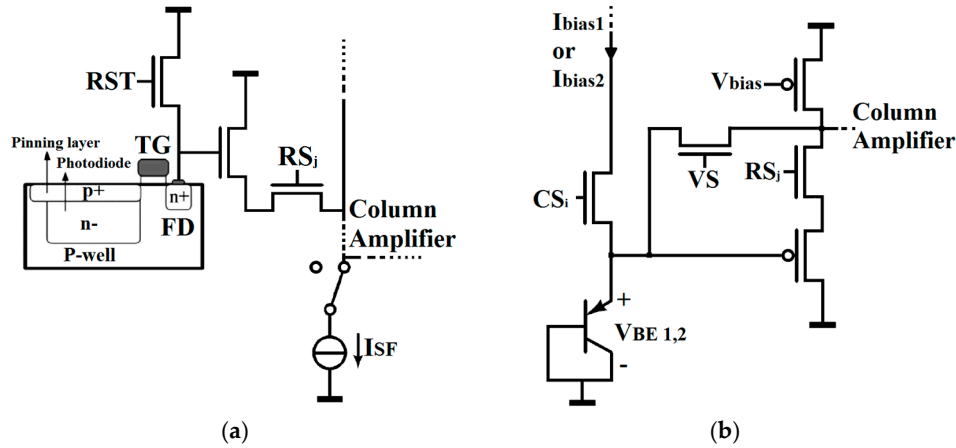


**Figure 1.** (a) Schematic of the CMOS 4T pixel; (b) Schematic of the temperature sensor pixel. Signal VS should be on to read the base emitter voltage.

The test chips have been fabricated by a standard 0.18  $\mu\text{m}$  CMOS Image Sensor (CIS) TowerJazz Technology.

### 2.2. Readout System

Pixels and Tixels use the same control signals and readout structure. The readout system is composed of row-column decoders, a biasing circuit, column amplifiers and output buffers, as shown in Figure 2. The decoders are used to select the pixels and Tixels position in the array. The Tixel is biased by a current source provided by the bias circuit. The bias circuit has a current mirror which is biased by an external current source of 1  $\mu\text{A}$ . This bias circuit is able to provide current ratios 4:1, 3:1, and 2:1. At the same time, the column amplifier consists of a Programmable Gain Amplifier (PGA) and the Correlated Double Sampling (CDS). The PGA provides gains between [1, 2, 4, 8, 16]. The output buffer connects the output signal to, in this case, an off-chip ADC to obtain the data.

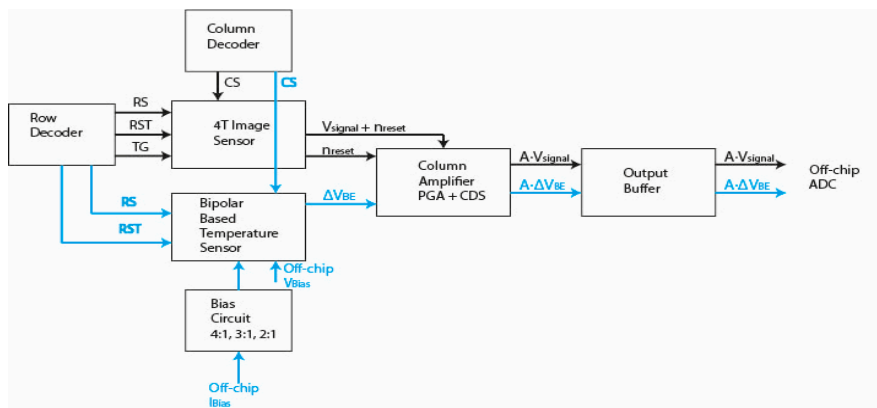


**Figure 2.** Block diagram of the readout system.

### 3. Measurements

The data of the image sensor is obtained by using an external 16 bits ADC (AD9826) connected to the output buffer. The control signals of the chip are generated by using a FPGA and the data coming from the ADC is saved in an Excel file generated in LabView. The data is processed by using Matlab. In total 100 frames are taken for both, pixels and Tixels.

#### 3.1. Image Sensor

The pixels of the image sensor have been tested. Figure 3a shows a chip micro-photograph and (b) a photo taken by the image sensor.

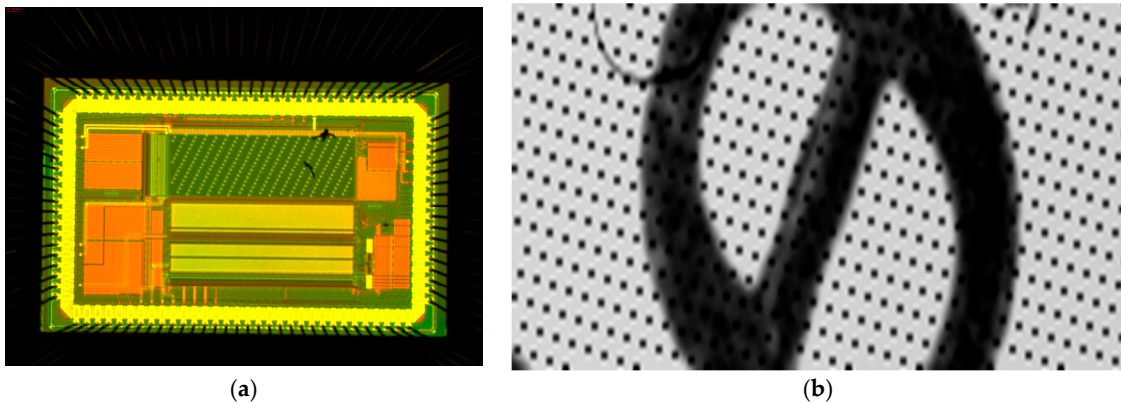


Figure 3. (a) Microphotograph of the text chip; (b) Photo taken by using the image sensor.

As we can see in Figure 3b, the image sensor is able to take a picture and it is possible to recognize the Tixels as the black dots along the picture.

#### 3.2. Temperature Sensors

The Tixels have been characterized by using a temperature control oven Vötsch model VT7004 in a range of [20 to 90] °C. The chip has been placed on a large aluminum block to stabilize the temperature and an accuracy of 0.015 °C has been reached. The temperature sensor signals have been averaged over 100 frames and 555 Tixels. The measurements have been done by using two gains: Gain 16 (G16) and Gain 8 (G8). Figure 4a shows the temperature conversion of the output voltage using G16 and Figure 4b shows the temperature error after 1st order best curve fitting. 555 Tixels have been averaged.

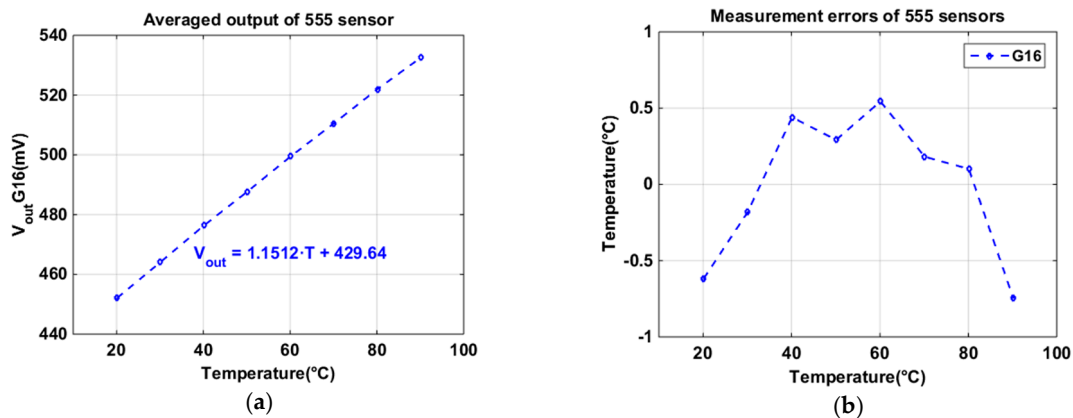
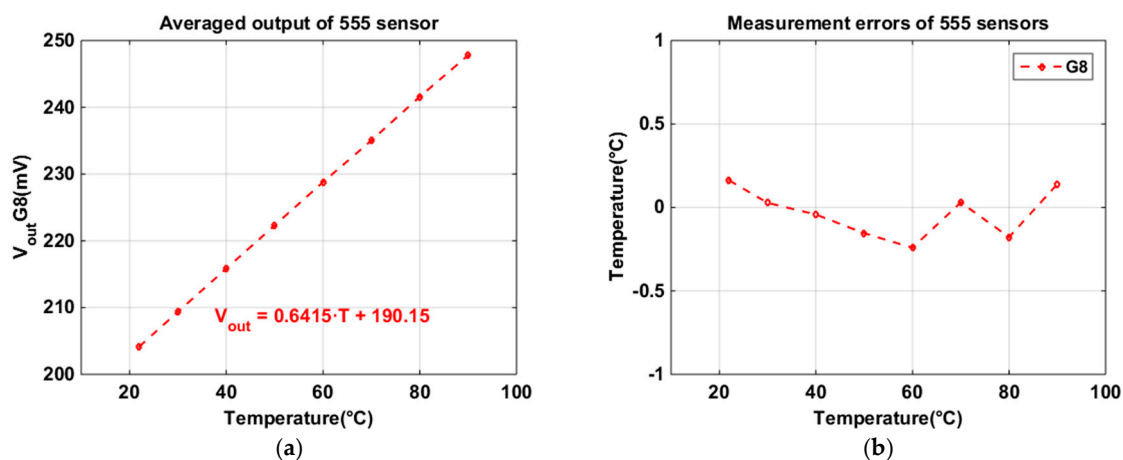


Figure 4. (a) Temperature sweep using G16. It shows the temperature coefficient; (b) Temperature error after first order best curve fitting.

Figure 5a shows the temperature conversion of the output voltage using G8 and Figure 5b shows the temperature error after 1st order best curve fitting.



**Figure 5.** (a) Temperature sweep using G16. It shows the temperature coefficient; (b) Temperature error after first order best curve fitting.

The output voltage vs. temperature of G16 exhibits a high linearity ( $R^2 = 0.9996$ ) in the temperature range [20 to 90] °C. The maximum error after first order best curve fitting in the case of G16 is 0.7 °C. In the case of G8, it also shows a high linearity ( $R^2 = 0.9999$ ) in this temperature range having a maximum error (1st order best curve fitting) of 0.3 °C.

#### 4. Conclusions

An image sensor composed of pixels and temperature sensors has been designed and fabricated. Both pixels and Tixels are placed in the active imaging array and use the same readout circuit. Results prove the concept of using the same readout circuit for measuring both sensor types. The output voltage vs. temperature shows a temperature coefficient of 1.1512 mV/°C in the case of G16 and 0.6415 mV/°C for G8. Temperature sensors show errors in the order of 0.7 °C (G16) and 0.3 °C (G8) in a temperature range [20 to 90] °C.

**Acknowledgments:** The authors acknowledge TowerJazz for the prototype CIS devices. The research is part of the CISTERN project, funded by the Dutch Government.

**Conflicts of Interest:** The authors declare no conflict of interest.

#### References

1. Wang, X. Noise in Sub-Micron CMOS Image Sensors. Ph.D. Thesis, Delft University of Technology, Delft, The Netherlands, 3 November 2008; pp. 46–68.
2. Baranov, P.S.; Litvin, V.T.; Belous, D.A.; Mantsvetov, A.A. Dark Current of the Solid-State Imagers at High Temperature. In Proceedings of the EIConRus IEEE Conference of Russian, Saint Petersburg, Russia, 1–3 February 2017; pp. 635–638.
3. Fossum, E.R.; Hondongwa, D.B. A Review of the Pinned Photodiode for CCD and CMOS Image Sensors. *IEEE J. Electron Devices Soc.* **2014**, *2*, 33–43, doi:10.1109/JEDS.2014.2306412.
4. Souri, K.; Chae, Y.; Makinwa, K. A CMOS Temperature Sensor with a Voltage-Calibrated Inaccuracy of  $\pm 0.15$  °C ( $3\sigma$ ) from  $-55$  °C to  $125$  °C. *IEEE J. Solid State Circuits* **2013**, *48*, 292–301, doi:10.1109/JSSC.2012.2214831.
5. Meijer, G.C.; Wang, G.; Fruett, F. Temperature Sensors and Voltage References Implemented in CMOS Technology. *IEEE Sens. J.* **2001**, *1*, 225–234, doi:10.1109/JSEN.2001.954835.

